Inhibition of Rho A activity causes pemphigus skin blistering

Jens Waschke,[1] Volker Spindler,[1] Paola Bruggeman,[1] Detlef Zillikens,[2] Gudula Schmidt,[3] and Detlev Drenckhahn[1]

[1]Institute of Anatomy and Cell Biology, University of Würzburg, D-97070 Würzburg, Germany
[2]Department of Dermatology, University of Lübeck, D-23538 Luebeck, Germany
[3]Department of Pharmacology and Toxicology, University of Freiburg, D-79104 Freiburg, Germany

The autoimmune blistering skin diseases pemphigus vulgaris (PV) and pemphigus foliaceus (PF) are mainly caused by autoantibodies against desmosomal cadherins. In this study, we provide evidence that PV–immunoglobulin G (IgG) and PF-IgG induce skin blistering by interference with Rho A signaling. In vitro, pemphigus IgG caused typical hallmarks of pemphigus pathogenesis such as epidermal blistering in human skin, cell dissociation, and loss of desmoglein 1 (Dsg 1)–mediated binding probed by laser tweezers. These changes were accompanied by interference with Rho A activation and reduction of Rho A activity. Pemphigus IgG–triggered keratinocyte dissociation and Rho A inactivation were p38 mitogen-activated protein kinase dependent. Specific activation of Rho A by cytotoxic necrotizing factor-y abolished all pemphigus-triggered effects, including keratin retraction and release of Dsg 3 from the cytoskeleton. These data demonstrate that Rho A is involved in the regulation of desmosomal adhesion, at least in part by maintaining the cytoskeletal anchorage of desmosomal proteins. This may open the possibility of pemphigus treatment with the epidermal application of Rho A agonists.

Introduction

The autoimmune blistering skin diseases pemphigus vulgaris (PV) and pemphigus foliaceus (PF) are caused by autoantibodies (IgG) against desmosomal cadherins and different antigens, including cholinergic receptors (Hu et al., 1978; Amagai et al., 1991, 1995; Nguyen et al., 2000; Sitaru and Zillikens, 2005). We have previously shown that PF-IgG caused cellular dissociation without directly inhibiting desmoglein (Dsg) 1 binding when probed by laser tweezers and atomic force microscopy (Waschke et al., 2005a). These data favor the contribution of cellular signaling rather than a direct inhibitory action on Dsg binding.

To investigate signaling events in pemphigus blistering, we used an ex vivo human skin model (Schiltz and Michel, 1976; Hu et al., 1978) and the human epidermal cell line HaCaT. We focused on Rho GTPases in this study because they are involved in the regulation of adhesion mediated by several members of the cadherin family (Fukata et al., 1999), and we found that the inhibition of Rho GTPases by *Clostridium difficile* toxin B induced epidermal splitting similar to pemphigus IgG (unpublished data). However, the role of Rho GTPases in the control of desmosomal adhesion is unclear at present (Braga and Yap, 2005). A previous study reported that Rho proteins regulate epithelial cadherin (E-cadherin)–mediated adhesion but not the maintenance of desmosomes in keratinocytes because the microinjection of C3 toxin to inhibit Rho A and a constitutively inactive mutant of Rac 1 altered the localization of E-cadherin but not of desmoplakin, a component of the desmosomal plaques (Braga et al., 1997). However, it is possible that the short incubation period of 25 min after microinjection used in the study was sufficient to destabilize adherens junctions but not desmosomes. Thus, a definitive conclusion concerning the role of Rho GTPases in the regulation of desmosomal adhesion cannot be drawn from these studies. Our data demonstrate for the first time that Rho A is involved in the maintenance of desmosomes and that interference with Rho A signaling considerably contributes to pemphigus pathogenesis.

J. Waschke and V. Spindler contributed equally to this paper.

Correspondence to Jens Waschke: jens.waschke@mail.uni-wuerzburg.de

Abbreviations used in this paper: CNF, cytotoxic necrotizing factor; Dsg, desmoglein; E-cadherin, epithelial cadherin; F-actin, filamentous actin; PF, pemphigus foliaceus; PV, pemphigus vulgaris.

Results and discussion

Incubation of human skin for 24 h in the presence of PV- or PF-IgG caused epidermal splitting, whereas no epidermal splitting was found after incubation in the absence of patients' IgG or with IgG from a healthy volunteer (Fig. 1, A–C). PV-IgG1–induced splitting occurred suprabasally, whereas in the PF-IgG1–treated epidermis, the cleavage plane was found to be both deep

© The Rockefeller University Press $8.00
The Journal of Cell Biology, Vol. 175, No. 5, December 4, 2006 721–727
http://www.jcb.org/cgi/doi/10.1083/jcb.200605125

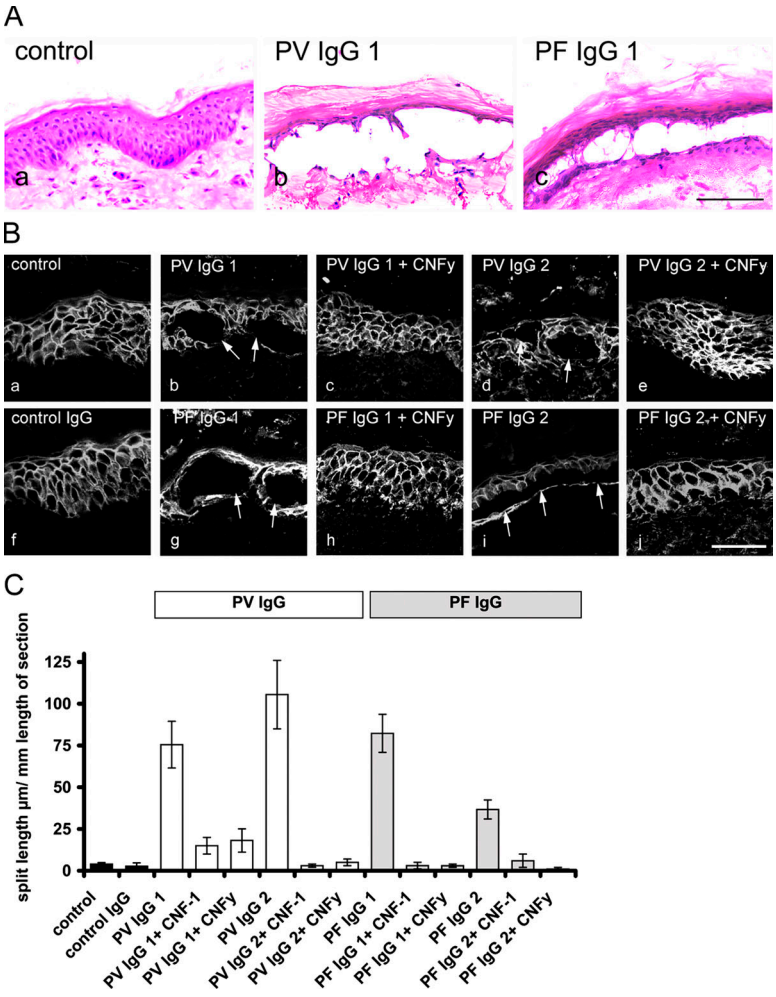

Figure 1. **Effect of Rho A activation on pemphigus IgG–induced epidermal splitting.** (A, a) Hematoxylin and eosin staining of human skin reveals no epidermal splitting in the absence of pemphigus IgG. (b and c) PV- and PF-IgG1–induced epidermal splitting after 24 h of incubation. Bar, 250 µm. (B, a) Dsg 3 is localized along cell junctions in human epidermis. (b–e) Epidermal splitting caused by PV-IgG1 and 2 (arrows; b and d) is inhibited by simultaneous CNFy-mediated activation of Rho GTPases. (f) Control IgG had no effect. (g–j) Splitting caused by PF-IgG1 and 2 (arrows; g and i) was also abrogated by CNFy. Bar, 50 µm. (C) PV-IgG1– and 2– as well as PF-IgG1– and 2–induced epidermal splitting (measured as the split length in micrometers relative to the length of the section in millimeters) was abolished by CNF-1 as well as by CNFy (the number of sections are as follows: 111 control, 28 control IgG, 50 PV-IgG1, 51 PV-IgG2, 24 PV-IgG1 + CNF-1, 26 PV-IgG1 + CNFy, 31 PV-IgG2 + CNF-1, 31 PV-IgG2 + CNFy, 37 PF-IgG1, 63 PF-IgG2, 35 PF-IgG1 + CNF-1, 32 PF-IgG1 + CNFy, 24 PF-IgG2 + CNF-1, and 30 PF-IgG2 + CNFy). Error bars represent SEM.

(not depicted) and within the spinous layer (Fig. 1 A). In control skin, Dsg 3 was localized along cell junctions throughout the entire epidermis except for the granular layer, which displayed weak staining (Fig. 1 B, a). We used two different bacterial toxins specific for Rho family GTPases: *Escherichia coli* cytotoxic necrotizing factor 1 (CNF-1), a toxin that activates Rho A, Rac 1, and Cdc42 by deamidation (Schmidt et al., 1997, 1998), as well as CNFy from *Yersinia pseudotuberculosis* because it selectively activates Rho A (Hoffmann et al., 2004). Selective activation of Rho A by CNFy was equally effective as activation of Rho A, Rac 1, and Cdc42 by CNF-1 to block pemphigus IgG–induced skin splitting (Fig. 1, B and C). From these data, we concluded that Rho A is the primary Rho GTPase targeted by pemphigus IgG–triggered signaling mechanisms.

To further test this hypothesis, we performed parallel experiments with cultured human keratinocytes (HaCaT) that, in contrast to the skin model, allow biophysical and biochemical studies. To detect pemphigus IgG–induced cell dissociation, we labeled the peripheral filamentous actin (F-actin) ring in HaCaT monolayers by Alexa-phalloidin staining. F-actin was enriched in a beltlike marginal zone along cell junctions (Fig. 2 a). After 24 h of incubation, PV-IgG1 (Fig. 2 b, arrows) as well as PF-IgG1 (Fig. 2 e, arrows) caused intercellular gap formation accompanied by the reorganization of F-actin from cellular junctions to a cytoplasmic meshwork. CNFy completely abolished pemphigus IgG–induced cell dissociation and actin reorganization and increased stress fiber formation along junctions (Fig. 2; c, d, and f). Similar results were obtained using PV- and PF-IgG2 (unpublished data). We studied the effects of pemphigus IgG on desmosome integrity by immunostaining for Dsg 3. In control cultures and monolayers incubated for 24 h in the presence of control IgG or CNFy, immunostaining for Dsg 3 remained localized to cell junctions (Fig. 3 A, a–c). Under the same conditions, PV-IgG2 and PF-IgG1 induced profound alterations of Dsg 3 immunolocalization (Fig. 3 A, e and i). In experiments using PF-IgG1, Dsg 3 staining remained continuously localized to cell junctions in areas where no gaps were present and was abolished at gap margins only (Fig. 3 A, i; arrows). Overall, changes induced by PV-IgG were stronger compared with effects induced by PF-IgG and ranged from the complete disappearance of Dsg 3 staining in some areas of the monolayer to substantial fragmentation of the continuous junction-associated Dsg 3 immunostaining (Fig. 3 A, e). Similar results were obtained using PV-IgG1 and PF-IgG2 (unpublished data).

Cell dissociation was observed with all patients' IgG fractions as well as after the inhibition of Rho A by a cell-permeable C3 fusion toxin for 24 h (Fig. 3 A, d). The latter finding is in contrast to an earlier study from Braga et al. (1997). In this study,

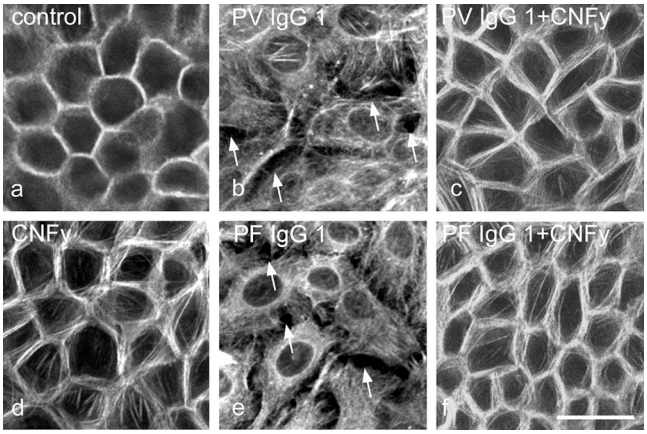

Figure 2. **Pemphigus-IgG–induced keratinocyte dissociation in HaCaT monolayers.** Alexa-phalloidin staining of actin filaments (F-actin) was used to sensitively detect cell dissociation. (a and b) Compared with controls, PV-IgG1 (24 h) caused cell dissociation (arrows) and profound alterations of F-actin distribution. (c) Cell dissociation was abolished by CNFy. (d) CNFy increased stress fibers along cell borders. (e and f) PF-IgG1–triggered cell dissociation (arrows; e) was inhibited by CNFy (f). $n = 5$. Bar, 35 μm.

the microinjection of C3 toxin to inhibit Rho A was found to displace E-cadherin from intercellular junctions in human keratinocytes, whereas the distribution of desmoplakin was not affected. From this result, it was concluded that Rho GTPases are not involved in the regulation of desmosomal adhesion. As outlined above, the failure of Rho A inhibition might be caused by the technical design of the study. When incubation with PV- and PF-IgG was performed in the presence of CNFy to selectively activate Rho A or with CNF-1, cellular dissociation and alteration of Dsg 3 staining in monolayers treated with PV-IgG2 (Fig. 3 A, f and g) or PF-IgG1 (Fig. 3 A, j and k) were almost completely abrogated. Similarly, the simultaneous inhibition of p38 MAPK by SB 202190 (Fig. 3 A, h and l) but not the inhibition of PKC by chelerythrine (not depicted) inhibited effects of PV-IgG2 and PF-IgG1, supporting recent findings from Berkowitz et al. (2005, 2006) both in vivo and in vitro. Collectively, these results indicate that autoantibody-induced keratinocyte dissociation in situ and in vitro as well as the loss of desmosomes in vitro can be suppressed by the activation of Rho A. Moreover, together with the observation that specific inhibition of Rho A by C3 fusion toxin also induced keratinocyte dissociation and the loss of desmosomes, these data demonstrate for the first time that the GTPase Rho A is critically involved in the maintenance of desmosomes.

Next, we tested the effect of pemphigus IgG and Rho A activation on the localization of desmoplakin and E-cadherin as well as on the keratin filament cytoskeleton. Compared with controls (Fig. 3 B, a–c), PV-IgG1 induced strong alterations of desmoplakin localization paralleled by keratin retraction, whereas the effects on the localization of E-cadherin and plakoglobin (not depicted) were less severe (Fig. 3 B, d–f; arrows pointing to the sides of cell dissociation). This is in line with previous studies describing desmoplakin fragmentation and keratin retraction (Caldelari et al., 2001; Calkins et al., 2006). However, when Rho A was activated by CNFy in the presence of PV-IgG1, the staining of desmoplakin and E-cadherin along

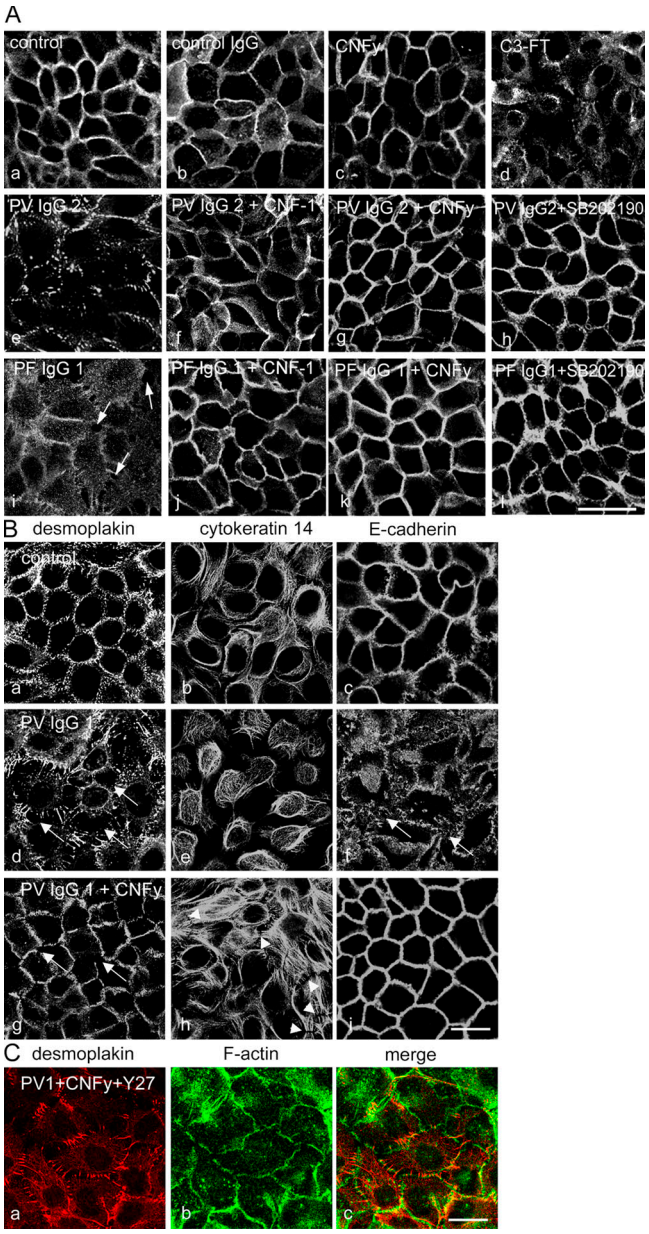

Figure 3. **Effects of pemphigus IgG and Rho A activation on the localization of desmosomal proteins, cytokeratin 14, and E-cadherin.** (A) HaCaT cells were stained for Dsg 3. (a–c) Continuous distribution of Dsg 3 along cell junctions in keratinocytes was not affected by control IgG or CNFy. (d) C3 fusion toxin caused cell dissociation and the loss of desmosomes. (e–h) The loss of Dsg 3 staining induced by PV-IgG2 (e) was blocked by either CNF-1 (f), CNFy (g), or SB 202190 (h). (i–l) Similarly, PF-IgG1–triggered intercellular gap formation (arrows; i) was inhibited by CNF-1 (j), CNFy (k), and SB 202190 (l). $n = 5$. Bar, 50 μm. (B) HaCaT monolayers were stained for desmoplakin (a, d, and g), cytokeratin 14 (b, e, and h), and E-cadherin (c, f, and i). (a–c) In controls, desmoplakin and E-cadherin were localized at cell junctions, whereas cytokeratin 14 displayed a cytoplasmic meshwork. (d–f) PV-IgG1 induced cell dissociation, with the loss of desmoplakin and E-cadherin staining (arrows) accompanied by keratin retraction. (g–i) Rho A activation by CNFy abolished cell dissociation and keratin retraction and largely reduced desmoplakin fragmentation (arrows). Under these conditions, cytokeratin 14 formed dense bundles perpendicular to cell junctions (arrowheads). (C) The effect of Rho kinase inhibition by Y27632 on the CNFy-mediated inhibition of PV-IgG1 was investigated by double staining for desmoplakin (a) and F-actin (b). (B and C) $n = 5$. Bars, 20 μm.

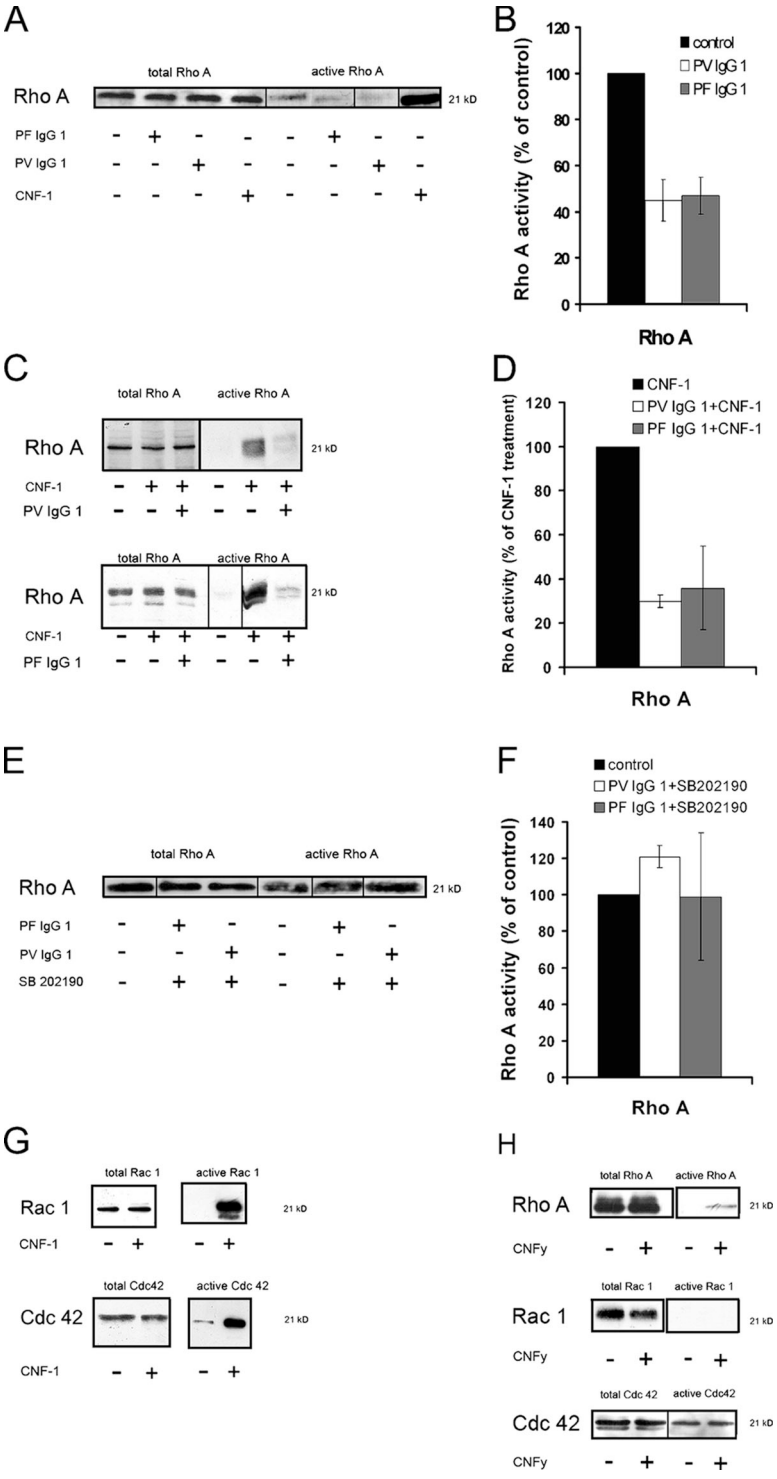

Figure 4. **Effect of pemphigus IgG on Rho A activity and activation.** Rho A activation assays were performed after incubation with PV- and PF-IgG1. Therefore, HaCaT cell lysates (indicating the total amount of the respective GTPase) and the pull-down fraction (indicating the active amount of the GTPase) were subjected to SDS-PAGE followed by Western blotting. The total content of Rho A was similar under all conditions. (A and B) PV- and PF-IgG1 reduced the activity of Rho A to ~50%. (C and D) Activation of Rho A by CNF-1 was reduced in the presence of pemphigus IgG. (E and F) SB 202190 inhibited Rho A inactivation by pemphigus IgG. (G and H) Besides Rho A, CNF-1 activated Rac 1 and Cdc42, whereas CNFy selectively activated Rho A. Note that as a result of the variable sensitivity of the activation assays, the activity of Rho A, Rac 1, and Cdc42 could not be determined under control conditions in all experiments (C, G, and H). The experiments shown are representative of three performed. Error bars represent SEM.

cell junctions was enhanced compared with controls (Fig. 3 B, g and j), and the fragmentation of desmoplakin was only rarely observed (Fig. 3 B, g; arrow). Under these conditions, keratin retraction was abolished, and many cells displayed dense keratin filament bundles running perpendicular to cell junctions (Fig. 3 B, h; arrowheads). Similar results were obtained using PV-IgG2 and PF-IgG1/2 (not depicted).

Inhibition of Rho kinase by Y27632 in addition to treatment with PV-IgG1 and CNFy partially blocked the protective effect of Rho activation on desmoplakin localization (Fig. 3 C, a and c), whereas the CNFy-induced inhibition of cell dissociation was not affected (Fig. 3 C, b and c), suggesting that Rho kinase is involved in some of the mechanisms regulated by Rho A. In summary, these data indicate that Rho A activation abrogates the pemphigus IgG–mediated disruption of desmosome anchorage to the keratin filament cytoskeleton.

On the basis of these results, we conclude that the activation of Rho A is sufficient to abrogate central events involved in

pemphigus blistering, like keratinocyte dissociation and epidermal splitting. To determine whether pemphigus IgG reduced the activity of Rho A in cultured HaCaT cells, we assayed Rho A activity by the ability of the GTPase to bind to the specific effector protein rhotekin coupled to agarose beads (Fig. 4). After incubation for 120 min, both PV- and PF-IgG1 reduced the amount of active Rho A to ~50% of control levels ($n = 3$; Fig. 4, A and B). Comparable results were obtained using PV- and PF-IgG2 (unpublished data). Next, we investigated whether the activation of Rho A was modified in response to pemphigus IgG because constant activation is required for Rho proteins to cycle between active and inactive states. When CNF-1 was applied together with PV- and PF-IgG1 for 120 min, the ability of CNF-1 to cause the activation of Rho A was decreased to 30 and 36% ($n = 3$) compared with cells treated with CNF-1 alone (Fig. 4, C and D).

Because the inhibition of p38 MAPK was equally efficient as Rho A activation to block pemphigus IgG–triggered keratinocyte dissociation, we investigated whether p38 MAPK was involved in Rho A inactivation in response to pemphigus IgG. When HaCaT monolayers were incubated with PV- and PF-IgG1 in the presence of the p38 MAPK inhibitor SB 202190, the IgG-triggered inactivation of Rho A was abolished (Fig. 4, E and F), indicating that p38 MAPK is part of the signaling cascade leading to Rho A inactivation. Finally, we proved that CNF-1 activated all three Rho proteins in human keratinocytes (i.e., Rho A [Fig. 4, A and B], Rac 1, and Cdc42 [Fig. 5 G]), whereas CNFy selectively activated Rho A (Fig. 4 H). Collectively, the results indicate that pemphigus IgG causes the inhibition of Rho A in a p38 MAPK–dependent manner, presumably by interference with GTPase activation.

We further characterized the mechanisms underlying Rho A–mediated maintenance of desmosomes and used the laser tweezer technique as a functional assay to study Dsg 1–mediated adhesion. In this assay, microbeads coated with recombinant Dsg 1 are allowed to settle on the surface of HaCaT cells for 30 min, where many beads undergo formation of desmosome-like cell to bead contacts as described previously (Waschke et al., 2005a). During this time course, typically ~65% of Dsg 1–coated beads had formed tight adhesive contacts and could no longer be displaced by the laser beam (Fig. 5 A). These control values were set to 100%. Adhesion of Dsg 1–coated beads was not significantly changed by incubation with control IgG for 120 min, whereas incubation with CNF-1 or CNFy increased the number of bound beads to 118 ± 5 and 122 ± 6%, respectively ($P < 0.05$). However, both the inhibition of Rho A by C3 fusion toxin (180 min) and the inhibition of Rho kinase by Y27632 for 180 min resulted in a significant reduction of bound beads to 52 ± 5 and 58 ± 4% of controls, respectively ($P < 0.05$). PV-IgG1 and 2 (120 min) also reduced bead binding to 82 ± 7 and 52 ± 5% of control levels. PV-IgG1– and 2–induced reduction of Dsg 1 binding was completely inhibited by simultaneous treatment of cultures with either CNF-1 or CNFy. Similarly, both CNF-1 and CNFy completely inhibited the weakening of bead binding caused by PF-IgG1 and 2. Thus, these experiments support our findings on cell dissociation in that the activation of Rho A alone is sufficient to prevent autoantibody-triggered weakening of Dsg 1–mediated adhesion. Because the specific

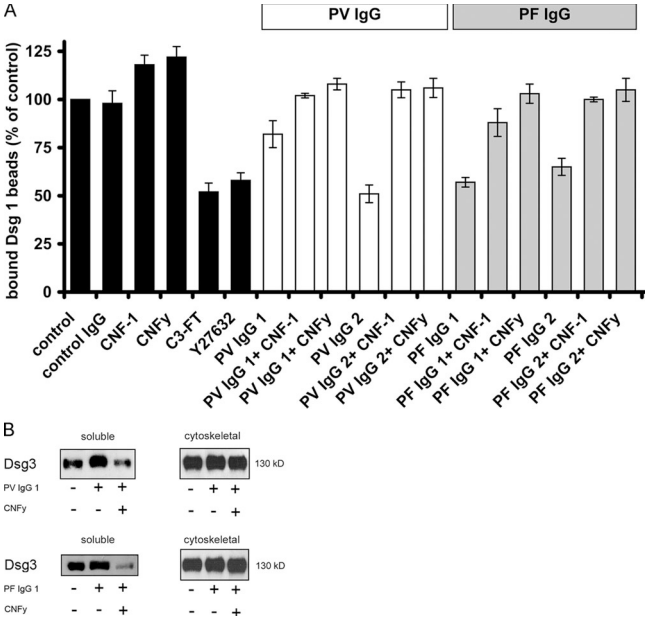

Figure 5. **Effect of Rho A activation on the pemphigus IgG–induced loss of Dsg 1–mediated binding and on the reduction of the cytoskeletal anchorage of Dsg 3.** (A) Dsg 1–coated microbeads were allowed to settle on the surface of HaCaT cells for 30 min and afterward were subjected to a laser beam. Beads not displaced by the laser beam were considered bound and set to 100% (controls). When added afterward, incubation with C3 fusion toxin or Y27632 reduced bead adhesion. PV-IgG1 and 2, PF-IgG1 and 2, or control IgG were applied alone or in the presence of CNF-1 or CNFy. PV- and PF-IgG significantly reduced the number of bound Dsg 1–coated beads, whereas control IgG had no effect ($P < 0.05$). However, the CNF-1–induced activation of Rho GTPases increased bead adhesion when applied alone and abrogated the reduction of Dsg 1 binding caused by pemphigus IgG. Specific activation of Rho A by CNFy was equally effective ($n = 6$ for each condition). (B) Cytoskeletal anchorage of Dsg 3 was assessed by Western blotting of the soluble and corresponding cytoskeletal fraction after incubation with pemphigus IgG in the absence or presence of CNFy. The experiments shown are representative of three performed. Error bars represent SEM.

inhibition of Rho A by C3 fusion toxin and the inhibition of Rho kinase also reduced Dsg 1 binding, we conclude that Rho A and Rho kinase are required for strong Dsg 1–mediated adhesion.

Our findings indicate that Rho A regulates the anchorage of desmosomes to the keratin filament cytoskeleton, which is required for strong Dsg 1 binding and maintenance of desmosomes. To test the cytoskeletal anchorage of desmosomal proteins, triton extraction can be used (Caldelari et al., 2001). Both PV- and PF-IgG1 increased Dsg 3 in the triton-soluble fraction of cell lysates, indicating that the anchorage of Dsg 3 to the cytoskeleton is reduced by pemphigus IgG (Fig. 5 B). Activation of Rho A by CNFy reversed the effects of PV- and PF-IgG1. Collectively, these data are consistent with our aforementioned results that the activation of Rho A blocked pemphigus IgG–induced keratin retraction and fragmentation of Dsg 3 and desmoplakin. Dsg 3 levels were not substantially decreased in the cytoskeletal fractions after 24 h of incubation with pemphigus IgG. This was similarly observed using higher concentrations (1 mg/ml) of patients' IgG (unpublished data). However, a recent study showed that Dsg 3 was substantially reduced after incubation with PV-IgG (Calkins et al., 2006), indicating that the mechanisms underlying pemphigus skin blistering are rather

complex and do not seem to be the same in different patients at all stages of the disease.

Collectively, we provide evidence that Rho A is critically involved in pemphigus pathogenesis and in the maintenance of desmosomes. However, at present, it is not clear how the inactivation of Rho proteins is induced by antibody binding. It is possible that signaling pathways caused by autoantibodies inhibit dissociation of the negative regulator Rho guanine nucleotide dissociation inhibitor from Rho A, thereby preventing GTP loading and making it ineffective to bind to its effector molecules. We found that the inactivation of Rho A was dependent on p38 MAPK, which is in line with a recent study (Berkowitz et al., 2005). Plakoglobin and PKC may also be involved in pemphigus pathogenesis (Seishima et al., 1999; Caldelari et al., 2001; Sanchez-Carpintero et al., 2004). Moreover, the precise mechanisms by which Rho A regulates desmosomal adhesion remain to be elucidated. We demonstrate that Rho A regulates the anchorage of desmosomal proteins to the keratin filament cytoskeleton. Finally, Rho A and Rho kinase seem to be required to provide strong Dsg 1 binding. Because Rho A activation inhibits the blistering effects of pemphigus IgG in human epidermis, this might be used as a new therapeutic approach with the possibility of topical epidermal application. Future studies are required to test whether Rho A activation by different approaches is effective in vivo.

Materials and methods

Cell culture and test reagents

HaCaT cells were cultured as described previously and were used for all experiments when grown to confluent monolayers (Waschke et al., 2005a). CNF-1 and CNFy were prepared and characterized as described previously (Schmidt et al., 1997, 1998; Hoffmann et al., 2004). Preliminary experiments indicated that CNF-1 at a dose of 300 ng/ml for 120 min and CNFy at a dose of 600 ng/ml for 6 h were necessary to induce the activation of Rho proteins (Waschke et al., 2006). For experiments using human epidermis, 1,200 ng/ml of both toxins were required. The cell-permeable C3 fusion toxin was a gift from H. Barth (University of Ulm, Ulm, Germany) and was used at 300 ng/ml for 180 min. Y27632 (Calbiochem) was used at 30 μM, and p38 MAPK inhibitor SB 202190 (Calbiochem) was applied at 10 μM. The specific inhibitor of PKC, chelerythrine (Sigma-Aldrich), was used at 10 μM.

Purification of PF-IgG

Sera from two PF patients and two patients suffering from a mucocutaneous form of PV whose diagnosis was confirmed clinically, histologically, and serologically and from a volunteer without any skin disease (control) were used for this study. Patients' sera were tested by ELISA for reactivity against Dsg 1 and 3, respectively. All sera contained Dsg 1 antibodies, whereas Dsg 3 antibodies were only present in PV-IgG fractions. Purification was performed as described previously (Waschke et al., 2005a). Concentrations of all IgG fractions were adjusted to a 150-μg/ml final concentration for all experiments.

Ex vivo model of human skin splitting

The model is similar to the technique established previously (Schiltz and Michel, 1976; Hu et al., 1978). Skin pieces were taken from fresh cadavers of individuals not suffering from any skin disease who had donated their bodies to the Institute of Anatomy and Cell Biology of Würzburg. Viability of the epidermis after incubation in DME at 37°C in the absence and presence of PV-IgG was confirmed by incubation with 3-[4,5-dimethylthiazol-2-yl]-2,5-diphenyl-tetrazolim bromide (MTT; Sigma-Aldrich) for 30 min, which was converted to a colored formazan by mitochondrial dehydrogenases using heat-inactivated epidermis (65°C for 30 min) as a negative control (Cole, 1986). Specimens were incubated with DME containing 10% FCS and 1.8 mM Ca^{2+} for 24 h in the presence or absence of PV- or PF-IgG alone or in combination with 1,200 ng/ml CNF-1 or CNFy. After brief rinsing with PBS (consisting of 137 mM NaCl, 2.7 mM KCl, 8.1 mM Na_2HPO_4, and 1.5 mM KH_2PO_4, pH 7.4), skin specimens were mounted on copper plates using Reichert-Jung mounting medium (Cambridge Instruments) and frozen in liquid nitrogen. 5-μm–thick cryosections were obtained using a cryostat (Reichert-Jung 2800 Frigocut; Cambridge Instruments). Cryosections were stained with hematoxylin and eosin for histomorphological evaluation. For each condition, three to five pieces of skin (2 × 2 mm) from at least two different cadavers were used and incubated in the presence or absence of patients' IgG separately. From three to five skin pieces, 24–111 different sections were evaluated under the various conditions (numbers of sections evaluated for each condition are given in the figure legends). After each section harvested, at least 50 μm of tissue were discarded. In the next section, it was verified by microscopic evaluation that no epidermal splitting was found to ensure that each blister measured was counted not more than once. For each blister, the total split length was measured and normalized to the length of the specific section given in millimeters.

Cytochemistry

After incubation with autoantibodies, immunostaining was performed as described previously (Waschke et al., 2005a). After fixation with ice-cold acetone for 2 min and incubation with normal goat serum and 1% BSA at RT, monolayers were incubated for 16 h at 4°C with mouse monoclonal antibody directed to Dsg 3 (Zytomed), rabbit polyclonal to desmoplakin (Biozol), mouse monoclonal to cytokeratin 14 (Chemicon), or mouse monoclonal to E-cadherin (BD Transduction Laboratories; each dilution was 1:100 in PBS). After several rinses with PBS (three times for 5 min each), monolayers were incubated for 60 min at RT with Cy3-labeled secondary antibodies (Dianova). For the visualization of F-actin, Alexa-phalloidin (Invitrogen) diluted 1:60 in PBS was used (incubation for 1 h at RT). Cells incubated with antibodies or Alexa-phalloidin were rinsed with PBS (three times for 5 min each).

Laser tweezer

The expression and purification of recombinant Dsg 1, coating of polystyrene beads, and the laser tweezer setup were described previously (Waschke et al., 2005a). Throughout all experiments, the laser intensity was 42 mW in the focal plane. Coated beads (10 μl of stock solution) were suspended in 200 μl of culture medium and allowed to interact with HaCaT monolayers for 30 min at 37°C before measuring the number of bound beads (equal to control values). Beads were considered tightly bound when resisting laser displacement at a 42-mW setting. For every condition, 100 beads were counted. Afterward, control IgG, PV-IgG, or PF-IgG were applied under various conditions for 120 min, and the number of bound beads was counted again. The percentage of beads resisting laser displacement under various experimental conditions was normalized to control values.

Rho protein activation assay

To test the effect of pemphigus IgG on the activation of Rho proteins, HaCaT cells were treated with either PF-IgG, PV-IgG, CNF-1, CNFy, or SB 202190 alone or in combinations as indicated before cells were subjected to activation assay kits for Rho A (Upstate Biotechnology), which were applied according to the manufacturer's instructions. The technique was used as described previously (Waschke et al., 2006).

Protein extraction

Extraction, Western blotting, and immunodetection were essentially performed as described previously (Waschke et al., 2005b) with the following exceptions. HaCaT cells were grown to full confluence in six-well dishes. After incubation with pemphigus IgG in the absence or presence of CNFy, monolayers were incubated with extraction buffer (1% Triton X-100, 10 mM Tris, 140 mM NaCl, 5 mM EDTA, and 2 mM EGTA) containing protease inhibitor solution (20 μg/ml each of leupetin, pepstatin, and aprotinin and 1 mM PMSF; all were obtained from Sigma-Aldrich) for 10 min on ice. Cells were scraped, vortexed briefly, and centrifuged at 14,000 *g* for 30 min. The supernatant was collected and defined as the Triton-soluble fraction. The pellet was defined as the cytoskeletal fraction and dissolved immediately in 10% SDS-containing sample buffer at 95°C for 5 min. Finally, immunodetection was performed using mouse monoclonal Dsg 3 antibody (Zytomed) diluted 1: 1,000 in PBS.

Image acquisition and manipulation

The histology and immunofluorescent images were taken with a microscope (LSM 510; Carl Zeiss MicroImaging, Inc.) using 40× NA 1.3 oil plan Neofluar and 63× NA 1.4 oil plan Apochromat objectives

(Carl Zeiss MicroImaging, Inc.). Images were taken by RT in antifade as an imaging medium for immunofluorescence and 80% glycerol for hematoxylin and eosin staining. The fluorochromes used were Cy3 and Alexa488. Densitometric quantification of Western blot bands was performed using Photoshop 7.0 software (Adobe). Photoshop 7.0 software was also used for the adjustment of contrast and brightness.

Statistics

Differences in bead adhesion and epidermal splitting were assessed using the *t* test. In text and bar diagrams, values were expressed as the mean ± SEM. Statistical significance was assumed for $P < 0.05$.

We thank Stefanie Imhof, Agnes Weth, and Marion Abele for excellent technical assistance. C3 fusion toxin was a gift of Holger Barth.

This study was supported by a grant from the Deutsche Forschungsgemeinschaft (SFB 487 [TP B5]). G. Schmidt is supported by grant SFB 388 (TP C7).

The authors have no conflicting financial interests.

Submitted: 19 May 2006
Accepted: 24 October 2006

References

Amagai, M., V. Klaus-Kovtun, and J.R. Stanley. 1991. Autoantibodies against a novel epithelial cadherin in pemphigus vulgaris, a disease of cell adhesion. *Cell*. 67:869–877.

Amagai, M., T. Hashimoto, K.J. Green, N. Shimizu, and T. Nishikawa. 1995. Antigen-specific immunoadsorption of pathogenic autoantibodies in pemphigus foliaceus. *J. Invest. Dermatol.* 104:895–901.

Berkowitz, P., P. Hu, Z. Liu, L.A. Diaz, J.J. Enghild, M.P. Chua, and D.S. Rubenstein. 2005. Desmosome signaling. Inhibition of p38MAPK prevents pemphigus vulgaris IgG-induced cytoskeleton reorganization. *J. Biol. Chem.* 280:23778–23784.

Berkowitz, P., P. Hu, S. Warren, Z. Liu, L.A. Diaz, and D.S. Rubenstein. 2006. p38MAPK inhibition prevents disease in pemphigus vulgaris mice. *Proc. Natl. Acad. Sci. USA*. 103:12855–12860.

Braga, V.M., and A.S. Yap. 2005. The challenges of abundance: epithelial junctions and small GTPase signalling. *Curr. Opin. Cell Biol.* 17:466–474.

Braga, V.M., L.M. Machesky, A. Hall, and N.A. Hotchin. 1997. The small GTPases Rho and Rac are required for the establishment of cadherin-dependent cell-cell contacts. *J. Cell Biol.* 137:1421–1431.

Caldelari, R., A. de Bruin, D. Baumann, M.M. Suter, C. Bierkamp, V. Balmer, and E. Muller. 2001. A central role for the armadillo protein plakoglobin in the autoimmune disease pemphigus vulgaris. *J. Cell Biol.* 153:823–834.

Calkins, C.C., S.V. Setzer, J.M. Jennings, S. Summers, K. Tsunoda, M. Amagai, and A.P. Kowalczyk. 2006. Desmoglein endocytosis and desmosome disassembly are coordinated responses to pemphigus autoantibodies. *J. Biol. Chem.* 281:7623–7634.

Cole, S.P. 1986. Rapid chemosensitivity testing of human lung tumor cells using the MTT assay. *Cancer Chemother. Pharmacol.* 17:259–263.

Fukata, M., M. Nakagawa, S. Kuroda, and K. Kaibuchi. 1999. Cell adhesion and Rho small GTPases. *J. Cell Sci.* 112:4491–4500.

Hoffmann, C., M. Pop, J. Leemhuis, J. Schirmer, K. Aktories, and G. Schmidt. 2004. The *Yersinia pseudotuberculosis* cytotoxic necrotizing factor (CNFY) selectively activates RhoA. *J. Biol. Chem.* 279:16026–16032.

Hu, C.H., B. Michel, and J.R. Schiltz. 1978. Epidermal acantholysis induced in vitro by pemphigus autoantibody. An ultrastructural study. *Am. J. Pathol.* 90:345–361.

Nguyen, V.T., A. Ndoye, L.D. Shultz, M.R. Pittelkow, and S.A. Grando. 2000. Antibodies against keratinocyte antigens other than desmogleins 1 and 3 can induce pemphigus vulgaris-like lesions. *J. Clin. Invest.* 106:1467–1479.

Sanchez-Carpintero, I., A. Espana, B. Pelacho, N. Lopez Moratalla, D.S. Rubenstein, L.A. Diaz, and M.J. Lopez-Zabalza. 2004. In vivo blockade of pemphigus vulgaris acantholysis by inhibition of intracellular signal transduction cascades. *Br. J. Dermatol.* 151:565–570.

Schiltz, J.R., and B. Michel. 1976. Production of epidermal acantholysis in normal human skin in vitro by the IgG fraction from pemphigus serum. *J. Invest. Dermatol.* 67:254–260.

Schmidt, G., P. Sehr, M. Wilm, J. Selzer, M. Mann, and K. Aktories. 1997. Gln 63 of Rho is deamidated by *Escherichia coli* cytotoxic necrotizing factor-1. *Nature*. 387:725–729.

Schmidt, G., J. Selzer, M. Lerm, and K. Aktories. 1998. The Rho-deamidating cytotoxic necrotizing factor 1 from *Escherichia coli* possesses transglutaminase activity. Cysteine 866 and histidine 881 are essential for enzyme activity. *J. Biol. Chem.* 273:13669–13674.

Seishima, M., Y. Iwasaki-Bessho, Y. Itoh, Y. Nozawa, M. Amagai, and Y. Kitajima. 1999. Phosphatidylcholine-specific phospholipase C, but not phospholipase D, is involved in pemphigus IgG-induced signal transduction. *Arch. Dermatol. Res.* 291:606–613.

Sitaru, C., and D. Zillikens. 2005. Mechanisms of blister induction by autoantibodies. *Exp. Dermatol.* 14:861–875.

Waschke, J., P. Bruggeman, W. Baumgartner, D. Zillikens, and D. Drenckhahn. 2005a. Pemphigus foliaceus IgG causes dissociation of desmoglein 1-containing junctions without blocking desmoglein 1 transinteraction. *J. Clin. Invest.* 115:3157–3165.

Waschke, J., F.E. Curry, R.H. Adamson, and D. Drenckhahn. 2005b. Regulation of actin dynamics is critical for endothelial barrier functions. *Am. J. Physiol. Heart Circ. Physiol.* 288:H1296–H1305.

Waschke, J., S. Burger, F.R. Curry, D. Drenckhahn, and R.H. Adamson. 2006. Activation of Rac-1 and Cdc42 stabilizes the microvascular endothelial barrier. *Histochem. Cell Biol.* 125:397–406.